

Published in final edited form as:

Ann N Y Acad Sci. 2008 March ; 1125: 129–136. doi:10.1196/annals.1419.015.

Enzymology of the Wood–Ljungdahl Pathway of Acetogenesis

Stephen W. Ragsdale

Department of Biological Chemistry, University of Michigan, Ann Arbor, Michigan, USA

Abstract

The biochemistry of acetogenesis is reviewed. The microbes that catalyze the reactions that are central to acetogenesis are described and the focus is on the enzymology of the process. These microbes play a key role in the global carbon cycle, producing over 10 trillion kilograms of acetic acid annually. Acetogens have the ability to anaerobically convert carbon dioxide and CO into acetyl-CoA by the Wood–Ljungdahl pathway, which is linked to energy conservation. They also can convert the six carbons of glucose stoichiometrically into 3 mol of acetate using this pathway. Acetogens and other anaerobic microbes (e.g., sulfate reducers and methanogens) use the Wood–Ljungdahl pathway for cell carbon synthesis. Important enzymes in this pathway that are covered in this review are pyruvate ferredoxin oxidoreductase, CO dehydrogenase/acetyl-CoA synthase, a corrinoid iron-sulfur protein, a methyltransferase, and the enzymes involved in the conversion of carbon dioxide to methyl-tetrahydrofolate.

Keywords

acetogenic bacteria; carbon dioxide fixation; carbon monoxide; cobalamin

Introduction

Some anaerobic microbes, including acetogenic bacteria and methanogenic archaea, convert CO₂ to cellular carbon by the Wood–Ljungdahl pathway (Fig. 1).^{1,2} The global importance of acetogens is covered fully in Harold Drake's chapter.³ Acetogenic bacteria use this pathway as their major means of generating energy for growth. *Moorella thermoacetica*, isolated in 1942,⁴ is the model acetogen and is the organism on which most studies of the Wood–Ljungdahl have been performed; its genome was recently sequenced. Methanogens growing on H₂/CO₂ use the pathway for generating cell carbon; however, those that can grow on acetate, essentially run the pathway in reverse and generate energy by oxidizing acetate to 2 mol of CO₂.⁵ Acetoclastic methanogens also convert acetate into acetyl-CoA for cell carbon synthesis through the combined actions of acetate kinase^{6,7} and phosphotransacetylase.⁸

The Wood–Ljungdahl pathway contains an *Eastern* (in red) and a *Western* (in blue) branch (Fig. 1), as originally described.⁹ The Eastern branch is essentially the folate-dependent one-carbon metabolic pathway that is present from bacteria to humans and recapitulated with methanopterin in methanogens. The Western branch is unique to acetogens, methanogens, and sulfate reducers, and exhibits novel mechanistic features. Acetogenic bacteria (e.g., acetogens or homoacetogens) synthesize acetic acid as their sole or primary metabolic end-

Address for correspondence: Stephen W. Ragsdale, University of Michigan Medical School, 1150 W. Medical Center Dr., 5301 MSRB III, Ann Arbor, MI 48109. sragdsal@umich.edu.

Conflict of Interest

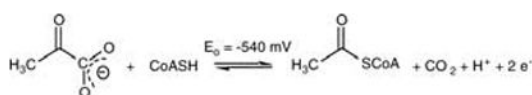
The author declares no conflicts of interest.

product. Globally, acetogens produce over 10^{13} kg (100 billion U.S. tons) of acetic acid annually,¹⁰ which dwarfs the total output of the world's chemical industry.

Figure 1 depicts growth of acetogens on glucose. However, these organisms can use a variety of substrates, including the biodegradation products of most natural polymers, such as cellulose, lignin (sugars, alcohols, aromatic compounds), and inorganic gases (CO , H_2 , CO_2). When acetogens grow on H_2/CO_2 , carbon enters the Wood–Ljungdahl pathway at the CO_2 reduction step, with H_2 serving as the electron donor. Acetogens are important in the biology of the soil, of extreme environments, and of organisms that house them in their digestive tract, such as humans, termites, and ruminants.^{11–13}

Pyruvate Ferredoxin Oxidoreductase

Pyruvate ferredoxin oxidoreductase (PFOR) was reviewed relatively recently.¹⁴ Catalyzing the oxidative decarboxylation of pyruvate to form acetyl-CoA and CO_2 , PFOR links heterotrophic metabolism to the Wood–Ljungdahl pathway (Fig. 1). PFOR is also key to cell carbon synthesis since, besides its catabolic function, PFOR catalyzes pyruvate formation by reductive carboxylation of acetyl-CoA.^{15,16} Pyruvate can then enter the incomplete tricarboxylic acid cycle^{17,18} to generate intermediates for cell carbon synthesis. PFOR is found in archaea, bacteria, and even anaerobic protozoa like *Giardia*.¹⁹



(1)

The structure of the *Desulfovibrio africanus* PFOR reveals seven domains.²⁰ Thiamine pyrophosphate (TPP) and a proximal [4Fe-4S] cluster (Cluster A) are deeply buried within the protein, while the other two clusters (B and C) lead to the surface (Fig. 2). The TPP binding site consists of two domains that bear strong structural similarity to those in other TPP enzymes²¹ and contains conserved residues that interact with Mg^{++} , pyrophosphate, and the thiazolium ring. Rapid kinetic studies indicate that the initial steps in oxidative decarboxylation of pyruvate by PFOR are similar to those of other TPP enzymes.²² Deprotonation of TPP yields the active ylide, which forms an adduct with pyruvate. Then, CO_2 is released, forming the 2α -hydroxyethylidene-TPP adduct (HE-TPP).²³ In acetogens, the CO_2 feeds into the Wood–Ljungdahl pathway^{24,25} (Fig. 1) and, based on isotope-exchange studies,²⁶ may be channeled directly to CO dehydrogenase/acetyl-CoA synthase (CODH/ACS).

After forming the HE-TPP intermediate, the negative charge on C-2 of HE-TPP promotes one-electron reduction of a proximal FeS cluster, forming an HE-TPP radical intermediate (Fig. 2). Based on the crystal structure, this intermediate was proposed to be a novel sigma-type acetyl radical²⁷; however, recent studies show that it is a pi radical with spin density delocalized over the aromatic thiazolium ring, as shown in the figure.^{28,29}

In the next step of the PFOR mechanism, the HE-TPP radical transfers an electron to the Fe-S electron-transfer chain, presumably through the oxidized A-cluster (Fig. 2). The rate of this electron-transfer reaction is CoA dependent.³⁰ In the absence of CoA, the half-life of the HE-TPP radical intermediate is ~2 min; however, in the presence of CoA, the rate of radical decay increases 100,000-fold.²² By studying various CoA analogues, it was shown that the thiol group of CoA alone lowers the transition state barrier for electron transfer by 40.5 kJ/

mol. The final step in the PFOR mechanism is electron transfer through Clusters A, B, and C (Fig. 2) to ferredoxin,²⁰ the terminal electron acceptor for PFOR. This electron-transfer reaction occurs extremely rapidly, with a second-order rate constant of $2\text{--}7 \times 10^7 \text{ M}^{-1} \text{ s}^{-1}$.^{22,31}

CODH/ACS

CODH/ACS was recently reviewed,³² so this part of the Wood–Ljungdahl pathway will be treated rather briefly. As shown in Figure 1, when acetogens are grown heterotrophically, the CO_2 and electrons generated by the PFOR reaction are utilized by CODH/ACS and formate dehydrogenase to generate CO and formate, respectively. When they are grown on CO, CODH generates CO_2 , which is then converted to formate in the Eastern branch of the pathway and CO is incorporated directly as the carbonyl group of acetyl-CoA. Both CO and CO_2 are unreactive without a catalyst, but the enzyme-catalyzed reactions are fast, with turnover numbers as high as $40,000 \text{ s}^{-1}$ reported for CO oxidation by the Ni-CODH from *Carboxydotherrmus hydrogenoformans* at its physiological growth temperature.³³ Even the least active CODHs catalyze CO oxidation at rates of $\sim 50 \text{ s}^{-1}$.³⁴ There are two major classes of CODHs: the aerobic Mo-Cu-Se CODH from carboxydobacteria and the Ni-CODHs. Found in aerobic bacteria that oxidize CO with O_2 ,^{35,36} the Mo-CODH contains FAD,³⁷ Fe/S centers, Cu, and 2 Mo atoms bound by molybdopterin cytosine dinucleotide, and its structure has been solved.³⁸ This enzyme will not be discussed further in this chapter, since only the Ni-CODH/ACS is involved in the Wood–Ljungdahl pathway. Ni-CODHs are divided into two classes: the monofunctional nickel CODH, which catalyzes the reaction shown in Equation 2, and the bifunctional CODH/ACS, which couples Equation 2 (CO formation) with Equation 3 (acetyl-CoA synthesis). The monofunctional CODH functions physiologically in the direction of CO oxidation, allowing microbes to take up and oxidize CO at the low levels found in the environment, while the CODH in the bifunctional protein converts CO_2 into acetyl-CoA.



The crystal structures of the monofunctional NI-CODH and the CODH component of the bifunctional enzymes are very similar.^{39–42} These mushroom-shaped, homodimeric enzymes contain five metal clusters per dimer: two C-clusters, two B-clusters, and a bridging D-cluster. The C-cluster is the catalytic site for CO oxidation and is buried 18 Å below the surface. This cluster can be described as a [3Fe-4S] cluster bridged to a binuclear NiFe cluster. The *Rhodospirillum rubrum* CODH structure with a bridging Cys between Ni and a special iron atom called ferrous component II (FCII), while the *C. hydrogenoformans* protein appears to have a sulfide bridge between Ni and FCII.^{43,44} Furthermore, there is evidence for a catalytically important persulfide at the C-cluster.⁴⁵ Issues related to the different structures are discussed in a recent review.⁴⁶ Cluster B is a typical $[\text{4Fe-4S}]^{2+/1+}$ cluster, while Cluster D is a $[\text{4Fe-4S}]^{2+/1+}$ cluster that bridges the two identical subunits, similar to the $[\text{4Fe-4S}]^{2+/1+}$ cluster in the iron protein of nitrogenase.

The CODH mechanism involves a Ping-Pong reaction: CODH is reduced by CO in the “ping” step and the reduced enzyme transfers electrons to an external redox mediator like ferredoxin in the “pong” step. The reduced electron acceptors then couple to other reduced

nicotinamide adenine dinucleotide phosphate (NAD(P)H) or ferredoxin-dependent cellular processes that require energy. Details of the CODH reaction have been reviewed.³² Recent studies of CODH linked to a pyrolytic graphite electrode show complete reversibility of CO oxidation and CO₂ reduction; in fact, at low pH values, the rate of CO₂ reduction exceeds that of CO oxidation.⁴⁷

The association of ACS with CODH forms a bi-functional CODH/ACS machine that is encoded by the *acsA/acsB* genes, respectively, and plays the key role in the Wood–Ljungdahl pathway.^{32,48,49} The CODH component catalyzes the conversion of CO₂ to CO (Eq. 2) to generate CO as a metabolic intermediate.²⁵ The CO₂ comes from the growth medium or from decarboxylation of pyruvate.^{25,30} Then, ACS catalyzes the condensation of CO,⁵⁰ CoA, and the methyl group of a methylated corrinoid iron–sulfur protein (CFeSP) to generate acetyl-CoA (Eq. 3),²⁵ a precursor of cellular material and a source of energy.

CODH/ACS contains a 140- \AA channel that delivers CO generated at the C-cluster to the A-cluster.^{40,51,52} The only metallocenter in ACS is the A-cluster, which consists of a [4Fe-4S] cluster bridged to a Ni site (Ni_p) that is thiolate bridged to another Ni ion in a thiolato-and carboxamido-type N₂S₂ coordination environment.^{40,42,53} Thus, one can describe the A-cluster as a binuclear NiNi center bridged by a cysteine residue (Cys509) to a [4Fe-4S] cluster, an arrangement similar to the Fe-Fe hydrogenases in which a [4Fe-4S] cluster and a binuclear Fe site are bridged by a Cys residue.^{87,88}

Two mechanisms for acetyl-CoA synthesis have been proposed that differ mainly in the electronic structure of the intermediates: one proposes a paramagnetic Ni(I)-CO species as a central intermediate,² and the other proposes a Ni(0) intermediate.^{54,55} A generic mechanism that emphasizes the organometallic nature of this reaction sequence is described in Figure 3.

Step 1, as shown in the figure, involves the migration of CO, derived from CO₂ reduction, through the inter-subunit channel to bind to the Ni_p site in the A-cluster. The binding of CO to ACS forms an organometallic complex, called the NiFeC species that has been characterized by a number of spectroscopic approaches.² The electronic structure of the NiFeC species is described as a [4Fe-4S]²⁺ cluster linked to a Ni¹⁺ center at the Ni_p site, while the other Ni apparently remains redox-inert in the Ni²⁺ state.⁵⁶ Lindahl's group has argued that the NiFeC species is not a true catalytic intermediate in acetyl-CoA synthesis, that it may represent an inhibited state, and that the Ni(0) state is the catalytically relevant one.^{54,55} See the recent review for a discussion of these issues.³² Step 2 in the ACS mechanism involves methylation of the A-cluster,⁵⁷ which involves the conversion of one organometallic species (methyl-Co) to another (methyl-Ni). There is evidence that the methyl group binds to the Ni_p site of the A-cluster.^{58–60} Carbon-carbon bond formation, Step 3 in the catalytic cycle, occurs by condensation of the methyl and carbonyl groups to form an acetyl-metal species. In the last step, CoA binds to ACS, triggering thiolysis of the acetyl-metal bond to form the C-S bond of acetyl-CoA, completing the reactions of the Western branch of the Wood–Ljungdahl pathway. Figure 3 indicates, for simplicity, that the ACS reaction sequence is ordered with CO binding before the methyl group. Conversely, Lindahl has argued for a strictly ordered binding mechanism, with methyl binding first, then CO, and finally CoA, as described in a recent review.⁵⁵ In the author's opinion, there is insufficient evidence to exclude the 1991 proposal that the carbonylation and methylation steps occur randomly⁶¹ (Fig. 4).

Tetrahydrofolate-Dependent Enzymes

Most of the work on the folate enzymes involved in the Eastern branch of the pathway has been performed in the Ljungdahl laboratory. The methyl group of acetyl-CoA is formed by

the six-electron reduction of CO₂ in the reactions of the Eastern branch of the acetyl-CoA pathway (Fig. 1).^{2,62} First, formate dehydrogenase converts CO₂ to formate,⁶³ which is condensed with H₄folate to form 10-formyl-H₄folate.^{64,65} The latter is then converted by a cyclohydrolase to 5,10-methenyl-H₄folate. Next, a dehydrogenase reduces methenyl- to 5,10-methylene-H₄folate,⁶⁶ which is reduced to (6S)-5-CH₃-H₄folate by a reductase.^{67,68}

Methyltransferase (MeTr, Acse) and Corrinoid Iron Sulfur Protein (CFeSP, AcsCD)

The methyl group of CH₃-H₄folate is transferred to the cobalt site in the cobalamin cofactor bound to the CFeSP^{69,70} to form an organometallic methyl-Co(III) intermediate in the Wood-Ljungdahl pathway (Fig. 1). This reaction is catalyzed by MeTr, encoded by the *acse* gene.²⁴ MeTr belongs to the B₁₂-dependent methyltransferase family that includes methionine synthase and related enzymes from methanogens.⁷¹ We have cloned, sequenced, and actively overexpressed MeTr^{72,73} and the CFeSP⁷⁴ in *E. coli*, making them amenable for site-directed mutagenesis studies. In collaboration with Cathy Drennan (MIT, Cambridge, Massachusetts), we also have determined the structure of MeTr and a site-directed variant in its uncomplexed⁷⁵ and CH₃-H₄folate-bound⁷⁶ states. It was concluded that CH₃-H₄folate binds tightly ($K_d < 10 \mu\text{M}$ ⁷⁷) to MeTr within a negatively charged crevice of the triose phosphate isomerase (TIM) barrel.⁷⁸ The structure of the CFeSP was also recently solved.⁷⁹

A key step in the MeTr mechanism is activation of the methyl group of CH₃-H₄folate, since the re-action involves displacement at a tertiary amine and because the CH₃-N bond is much stronger than the product CH₃-Co bond. Of the activation mechanisms that have been considered, protonation at N5 of the pterin seems to be most plausible.⁷¹ Generation of a positive charge on N5 would lower the activation barrier for nucleophilic displacement of the methyl group by the Co(I) nucleophile. There is significant experimental support for protonation at N5 of the pterin, including proton uptake studies,^{77,80} pH dependencies of the steady state, and transient reaction kinetics of MeTr⁸¹ and methionine synthase,⁸² and studies of variants that are compromised in acid-base catalysis.⁷⁶ A question that has not been resolved is whether the proton transfer takes place upon formation of the binary complex, as indicated by studies with MeTr from *M. thermoacetica*,^{49,77} or the ternary complex (with the methyl acceptor), as concluded from studies on *E. coli* methionine synthase.⁸⁰ Recent studies indicate that this protonation step relies on an H-bonding network, instead of a single acid-base catalyst and that an Asn residue is a key component of that network.⁷⁶

As shown in Figure 1, the CFeSP interfaces between CH₃-H₄folate/MeTr and CODH/ACS. This 88-kDa heterodimeric protein contains a [4Fe-S]^{2+/1+} cluster and a cobalt cobamide.^{70,74} The Fe-S cluster plays a role in reductive activation of the cobalt to the active Co(I) state.^{83,84} Svetlitchnaia *et al.*⁷⁹ proposed that the C-terminal domain (Fig. 5) of the large subunit is a mobile element that interacts alternatively with the A-cluster domain of ACS and with MeTr. Three major conformers or complexes are described: (1) a methylation complex, in which the Co(I)-CFeSP binds MeTr and accepts the methyl group of CH₃-H₄folate; (2) the methylated CFeSP; (3) a complex between ACS and the methylated CFeSP. A fourth conformation, which is not shown here, would be a reductive activation conformer, in which the corrinoid is in the inactive Co(II) state. This molecular juggling proposed for the CFeSP shown in Figure 5 has precedent in the related mechanism involving the various domains of methionine synthase, as shown by the elegant structure-function studies of Matthews and Ludwig.^{82,85,86}

Summary

Studies of the enzymes involved in the Wood–Ljungdahl pathway have elucidated new roles of metal ions in biology (including the formation of bioorganometallic intermediates, discovery of new heterometallic clusters, and nucleophilic metal ions), uncovered novel substrate-derived radical intermediates, and revealed channeling of gaseous substrates. These new outcomes and mechanisms will likely be applicable to other currently less well-studied metal-dependent enzyme systems. Now that detailed structures of PFOR, CODH/ACS, the CFeSP, and MeTr are available to provide a structural framework for these novel and important chemical reactions, mechanistic hypotheses can be posed and tested at a deeper level using a variety of biochemical and biophysical methods.

Acknowledgments

Work on the enzymology of acetogenesis has been funded by the NIH (GM39451). I am grateful for the contributions of Javier Seravalli and Elizabeth Pierce in my laboratory to the recent work on acetogenesis described here.

References

1. Ragsdale, SW. Metalloenzymes in the reduction of one-carbon compounds. In: Bertini, I., et al., editors. *Biological Inorganic Chemistry: Structure and Reactivity*. University Science Books; Mill Valley, CA: 2006. p. 452-467.
2. Ragsdale SW. Life with carbon monoxide. *CRC Crit Rev Biochem Mol Biol* 2004;39:165–195. [PubMed: 15596550]
3. Drake, HL. *Ann NY Acad Sci Incredible Anaerobes: From Physiology to Genomics to Fuels*. 2008. Old acetogens, new light. In Press
4. Fontaine FE, et al. A new type of glucose fermentation by *Clostridium thermoaceticum*. *J Bacteriol* 1942;43:701–715. [PubMed: 16560531]
5. Ferry JG. Biochemistry of methanogenesis. *Crit Rev Biochem Mol Biol* 1992;27:473–502. [PubMed: 1473352]
6. Ingram-Smith C, et al. Characterization of the acetate binding pocket in the Methanosarcina thermophila acetate kinase. *J Bacteriol* 2005;187:2386–2394. [PubMed: 15774882]
7. Gorrell A, et al. Structural and kinetic analyses of arginine residues in the active site of the acetate kinase from Methanosarcina thermophila. *J Biol Chem* 2005;280:10731–10742. [PubMed: 15647264]
8. Iyer PP, et al. Crystal structure of phosphotransacetylase from the methanogenic archaeon Methanosarcina thermophila. *Structure* 2004;12:559–567. [PubMed: 15062079]
9. Ragsdale SW. The Eastern and Western branches of the Wood/Ljungdahl pathway: how the East and West were won. *BioFactors* 1997;9:1–9.
10. Drake, HL., et al. Acetogenesis, acetogenic bacteria, and the acetyl-CoA pathway: past and current perspectives. In: Drake, HL., editor. *Acetogenesis*. Chapman and Hall; New York: 1994. p. 3-60.
11. Lajoie SF, et al. Acetate production from hydrogen and [¹³C]carbon dioxide by the microflora of human feces. *Appl Environ Microbiol* 1988;54:2723–2727. [PubMed: 3145708]
12. Breznak JA, et al. Acetate synthesis from H₂ plus CO₂ by termite gut microbes. *Appl Environ Microbiol* 1986;52:623–630. [PubMed: 16347157]
13. Breznak JA, et al. Microbial H₂/CO₂ acetogenesis in animal guts: nature and nutritional significance. *FEMS Microbiol, Rev* 1990;87:309–314. [PubMed: 2128799]
14. Ragsdale SW. Pyruvate:ferredoxin oxidoreductase and its radical intermediate. *Chem Rev* 2003;103:2333–2346. [PubMed: 12797832]
15. Furdui C, et al. The role of pyruvate:ferredoxin oxidoreductase in pyruvate synthesis during autotrophic growth by the Wood-Ljungdahl pathway. *J Biol Chem* 2000;275:28494–28499. [PubMed: 10878009]

16. Bock AK, et al. Catalytic properties, molecular composition and sequence alignments of pyruvate: ferredoxin oxidoreductase from the methanogenic archaeon *Methanosarcina barkeri* (strain Fusaro). *Eur J Biochem* 1996;237:35–44. [PubMed: 8620891]
17. Simpson, PG., et al. Anabolic pathways in methanogens. In: Ferry, JG., editor. *Methanogenesis: Ecology Physiology, Biochemistry & Genetics*. Chapman & Hall; London: 1993. p. 445–472.
18. Yoon KS, et al. Rubredoxin from the green sulfur bacterium *Chlorobium tepidum* functions as an electron acceptor for pyruvate ferredoxin oxidoreductase. *J Biol Chem* 1999;274:29772–29778. [PubMed: 10514453]
19. Horner DS, et al. A single eubacterial origin of eukaryotic pyruvate: ferredoxin oxidoreductase genes: Implications for the evolution of anaerobic eukaryotes. *Mol Biol Evol* 1999;16:1280–1291. [PubMed: 10486982]
20. Chabriere E, et al. Crystal structures of the key anaerobic enzyme pyruvate:ferredoxin oxidoreductase, free and in complex with pyruvate. *Nat Struct Biol* 1999;6:182–190. [PubMed: 10048931]
21. Muller YA, et al. A thiamin diphosphate binding fold revealed by comparison of the crystal structures of transketolase, pyruvate oxidase and pyruvate decarboxylase. *Structure* 1993;1:95–103. [PubMed: 8069629]
22. Furdui C, et al. The roles of coenzyme A in the pyruvate:ferredoxin oxidoreductase reaction mechanism: rate enhancement of electron transfer from a radical intermediate to an iron-sulfur cluster. *Biochemistry* 2002;41:9921–9937. [PubMed: 12146957]
23. Breslow R. Rapid deuterium exchange in thiazolium salts. *J Am Chem Soc* 1957;79:1762–1763.
24. Drake HL, et al. Purification of five components from *Clostridium thermoaceticum* which catalyze synthesis of acetate from pyruvate and methyltetrahydrofolate. Properties of phosphotransacetylase. *J Biol Chem* 1981;256:11137–11144. [PubMed: 7287757]
25. Menon S, et al. Evidence that carbon monoxide is an obligatory intermediate in anaerobic acetyl-CoA synthesis. *Biochemistry* 1996;35:12119–12125. [PubMed: 8810918]
26. Schulman M, et al. Total synthesis of acetate from CO₂. VII. Evidence with *Clostridium thermoaceticum* that the carboxyl of acetate is derived from the carboxyl of pyruvate by transcarboxylation and not by fixation of CO₂. *J Biol Chem* 1973;248:6255–6261. [PubMed: 4730320]
27. Chabriere E, et al. Crystal structure of the free radical intermediate of pyruvate:ferredoxin oxidoreductase. *Science* 2001;294:2559–2563. [PubMed: 11752578]
28. Mansoorabadi SO, et al. EPR spectroscopic and computational characterization of the hydroxyethylidene-thiamine pyrophosphate radical intermediate of pyruvate: ferredoxin oxidoreductase. *Biochemistry* 2006;45:7122–7131. [PubMed: 16752902]
29. Astashkin AV, et al. Pulsed electron paramagnetic resonance experiments identify the paramagnetic intermediates in the pyruvate ferredoxin oxidoreductase catalytic cycle. *J Am Chem Soc* 2006;128:3888–3889. [PubMed: 16551078]
30. Menon S, et al. Mechanism of the *Clostridium thermoaceticum* pyruvate:ferredoxin oxidoreductase: evidence for the common catalytic intermediacy of the hydroxyethylthiamine pyrophosphate radical. *Biochemistry* 1997;36:8484–8494. [PubMed: 9214293]
31. Pieulle L, et al. Structural and kinetic studies of the pyruvate-ferredoxin oxidoreductase/ferredoxin complex from *Desulfovibrio africanus*. *Eur J Biochem* 1999;264:500–508. [PubMed: 10491097]
32. Ragsdale SW. Nickel and the carbon cycle. *J Inorg Biochem* 2007;101:1657–1666. [PubMed: 17716738]
33. Svetlitchnyi V, et al. Two membrane-associated NiFeS-carbon monoxide dehydrogenases from the anaerobic carbon-monoxide-utilizing eubacterium *Carboxydotherrmus hydrogenoformans*. *J Bacteriol* 2001;183:5134–5144. [PubMed: 11489867]
34. Meyer O, et al. The role of Se, Mo and Fe in the structure and function of carbon monoxide dehydrogenase. *Biol Chem* 2000;381:865–876. [PubMed: 11076018]
35. Meyer, O., et al. Biochemistry of the aerobic utilization of carbon monoxide. In: Murrell, JC.; Kelly, DP., editors. *Microbial Growth on C₁ Compounds*. Intercept, Ltd; Andover, MA: 1993. p. 433–459.

36. Gnida M, et al. A novel binuclear [CuSMo] cluster at the active site of carbon monoxide dehydrogenase: characterization by X-ray absorption spectroscopy. *Biochemistry* 2003;42:222–230. [PubMed: 12515558]
37. Bates DM, et al. Substitution of leucine 28 with histidine in the Escherichia coli transcription factor FNR results in increased stability of the [4Fe-4S](2+) cluster to oxygen. *J Biol Chem* 2000;275:6234–6240. [PubMed: 10692418]
38. Dobbek H, et al. Crystal structure and mechanism of CO dehydrogenase, a molybdo iron-sulfur flavoprotein containing S-selenylcysteine. *Proc Natl Acad Sci USA* 1999;96:8884–8889. [PubMed: 10430865]
39. Drennan CL, et al. Life on carbon monoxide: X-ray structure of Rhodospirillum rubrum Ni-Fe-S carbon monoxide dehydrogenase. *Proc Natl Acad Sci USA* 2001;98:11973–11978. [PubMed: 11593006]
40. Doukov TI, et al. A Ni-Fe-Cu center in a bifunctional carbon monoxide dehydrogenase/acetyl-CoA synthase. *Science* 2002;298:567–572. [PubMed: 12386327]
41. Dobbek H, et al. Crystal structure of a carbon monoxide dehydrogenase reveals a [Ni-4Fe-5S] cluster. *Science* 2001;293:1281–1285. [PubMed: 11509720]
42. Darnault C, et al. Ni-Zn-[Fe(4)-S(4)] and Ni-Ni-[Fe(4)-S(4)] clusters in closed and open alpha subunits of acetyl-CoA synthase/carbon monoxide dehydrogenase. *Nat Struct Biol* 2003;10:271–279. [PubMed: 12627225]
43. Dobbek H, et al. Carbon monoxide induced decomposition of the active site [Ni-4Fe-5S] cluster of CO dehydrogenase. *J Am Chem Soc* 2004;126:5382–5387. [PubMed: 15113209]
44. Sun J, et al. Sulfur ligand substitution at the nickel(II) sites of cubane-type and cubanoid NiFe₃S₄ clusters relevant to the C-clusters of carbon monoxide dehydrogenase. *Inorg Chem* 2007;46:2691–2699. [PubMed: 17346040]
45. Kim EJ, et al. Evidence for a proton transfer network and a required persulfide-bond-forming cysteine residue in ni-containing carbon monoxide dehydrogenases. *Biochemistry* 2004;43:5728–5734. [PubMed: 15134447]
46. Drennan CL, et al. The metalloclusters of carbon monoxide dehydrogenase/acetyl-CoA synthase: a story in pictures. *J Biol Inorg Chem* 2004;9:511–515. [PubMed: 15221484]
47. Parkin A, et al. Rapid electrocatalytic CO₂/CO interconversions by Carboxydotherrmus hydrogenoformans CO dehydrogenase I on an electrode. *J Am Chem Soc* 2007;129:10328–10329. [PubMed: 17672466]
48. Fontecilla-Camps, J-C., et al. Nickel-iron-sulfur active sites: hydrogenase and CO dehydrogenase. In: Sykes, AG.; Cammack, R., editors. *Advances in Inorganic Chemistry*. Vol. 47. Academic Press, Inc; San Diego: 1999. p. 283-333.
49. Seravalli J, et al. Mechanism of transfer of the methyl group from (6S)-methyltetrahydrofolate to the corrinoid/iron-sulfur protein catalyzed by the methyl-transferase from Clostridium thermoaceticum: a key step in the Wood-Ljungdahl pathway of acetyl-CoA synthesis. *Biochemistry* 1999;38:5728–5735. [PubMed: 10231523]
50. Ragsdale SW, et al. EPR evidence for nickel substrate interaction in carbon monoxide dehydrogenase from *Clostridium thermoaceticum*. *Biochem Biophys Res Commun* 1982;108:658–663. [PubMed: 6293499]
51. Seravalli J, et al. Channeling of carbon monoxide during anaerobic carbon dioxide fixation. *Biochemistry* 2000;39:1274–1277. [PubMed: 10684606]
52. Maynard EL, et al. Evidence of a molecular tunnel connecting the active sites for CO₂ reduction and acetyl-CoA synthesis in acetyl-CoA synthase from *Clostridium thermoaceticum*. *J Am Chem Soc* 1999;121:9221–9222.
53. Svetlitchnyi V, et al. A functional Ni-Ni-[4Fe-4S] cluster in the monomeric acetyl-CoA synthase from Carboxydotherrmus hydrogenoformans. *Proc Natl Acad Sci USA* 2004;101:446–451. [PubMed: 14699043]
54. Bramlett MR, et al. Mossbauer and EPR study of recombinant acetyl-CoA synthase from Moorella thermoacetica. *Biochemistry* 2006;45:8674–8685. [PubMed: 16834342]
55. Lindahl PA. Acetyl-coenzyme A synthase: the case for a Ni⁰-Based mechanism of catalysis. *J Biol Inorg Chem* 2004;9:516–524. [PubMed: 15221478]

56. Brunold TC. Spectroscopic and computational insights into the geometric and electronic properties of the A cluster of acetyl-coenzyme A synthase. *J Biol Inorg Chem* 2004;9:533–541. [PubMed: 15221480]
57. Seravalli J, et al. Rapid kinetic studies of acetyl-CoA synthesis: evidence supporting the catalytic intermediacy of a paramagnetic NiFeC species in the autotrophic Wood-Ljungdahl pathway. *Biochemistry* 2002;41:1807–1819. [PubMed: 11827525]
58. Shin W, et al. Heterogeneous nickel environments in carbon monoxide dehydrogenase from *Clostridium thermoaceticum*. *J Am Chem Soc* 1993;115:5522–5526.
59. Barondeau DP, et al. Methylation of carbon monoxide dehydrogenase from *Clostridium thermoaceticum* and mechanism of acetyl coenzyme A synthesis. *J Am Chem Soc* 1997;119:3959–3970.
60. Seravalli J, et al. Evidence that Ni-Ni acetyl-CoA synthase is active and that the Cu-Ni enzyme is not. *Biochemistry* 2004;43:3944–3955. [PubMed: 15049702]
61. Lu WP, et al. Reductive activation of the coenzyme A/acetyl-CoA isotopic exchange reaction catalyzed by carbon monoxide dehydrogenase from *Clostridium thermoaceticum* and its inhibition by nitrous oxide and carbon monoxide. *J Biol Chem* 1991;266:3554–3564. [PubMed: 1995618]
62. Ragsdale SW. Enzymology of the acetyl-CoA pathway of CO₂ fixation. *CRC Crit Rev Biochem Mol Biol* 1991;26:261–300. [PubMed: 1935170]
63. Ljungdahl LG, et al. Formate dehydrogenase, a selenium-tungsten enzyme from *Clostridium thermoaceticum*. *Methods Enzymol* 1978;53:360–372. [PubMed: 713844]
64. Lovell CR, et al. Cloning and expression in *Escherichia coli* of the *Clostridium thermoaceticum* gene encoding thermostable formyltetrahydrofolate synthetase. *Arch Microbiol* 1988;149:280–285. [PubMed: 2833195]
65. Lovell CR, et al. Primary structure of the thermostable formyltetrahydrofolate synthetase from *Clostridium thermoaceticum*. *Biochemistry* 1990;29:5687–5694. [PubMed: 2200509]
66. Moore MR, et al. Purification and characterization of nicotinamide adenine dinucleotide-dependent methylenetetrahydrofolate dehydrogenase from *Clostridium formicoaceticum*. *J Biol Chem* 1974;249:5250–5253. [PubMed: 4153026]
67. Clark JE, et al. Purification and properties of 5,10-methylenetetrahydrofolate reductase, an iron-sulfur flavoprotein from *Clostridium formicoaceticum*. *J Biol Chem* 1984;259:10845–10889. [PubMed: 6381490]
68. Park, EY., et al. 5,10-methylenetetrahydrofolate reductases: iron-sulfur-zinc flavoproteins of two acetogenic clostridia. In: Miller, F., editor. *Chemistry and Biochemistry of Flavoenzymes*. Vol. 1. CRC Press; Boca Raton, FL: 1991. p. 389–400.
69. Hu SI, et al. Acetate synthesis from carbon monoxide by *Clostridium thermoaceticum*. Purification of the corrinoid protein. *J Biol Chem* 1984;259:8892–8897. [PubMed: 6746629]
70. Ragsdale SW, et al. Mössbauer, EPR, and optical studies of the corrinoid/Fe-S protein involved in the synthesis of acetyl-CoA by *Clostridium thermoaceticum*. *J Biol Chem* 1987;262:14289–14297. [PubMed: 2821001]
71. Banerjee R, et al. The many faces of vitamin B₁₂: catalysis by cobalamin-dependent enzymes. *Ann Rev Biochem* 2003;72:209–247. [PubMed: 14527323]
72. Roberts DL, et al. Cloning and expression of the gene cluster encoding key proteins involved in acetyl-CoA synthesis in *Clostridium thermoaceticum*: CO dehydrogenase, the corrinoid/Fe-S protein, and methyltransferase. *Proc Natl Acad Sci USA* 1989;86:32–36. [PubMed: 2911576]
73. Roberts DL, et al. The reductive acetyl-CoA pathway: sequence and heterologous expression of active CH₃-H₄folate:corrinoid/iron sulfur protein methyltransferase from *Clostridium thermoaceticum*. *J Bacteriol* 1994;176:6127–6130. [PubMed: 7928975]
74. Lu WP, et al. Sequence and expression of the gene encoding the corrinoid/iron-sulfur protein from *Clostridium thermoaceticum* and reconstitution of the recombinant protein to full activity. *J Biol Chem* 1993;268:5605–5614. [PubMed: 8449924]
75. Doukov T, et al. Preliminary X-ray diffraction analysis of the methyltetrahydrofolate:corrinoid/iron sulfur protein methyltransferase from *Clostridium thermoaceticum*. *Acta Crystallographa D51: Part* 1995;6:1092–1093.

76. Doukov TI, et al. Structural and kinetic evidence for an extended hydrogen bonding network in catalysis of methyl group transfer: role of an active site asparagine residue in activation of methyl transfer by methyltransferases. *J Biol Chem* 2007;282:6609–6618. [PubMed: 17172470]
77. Seravalli J, et al. Binding of (6R,S)-methyltetrahydrofolate to methyltransferase from *Clostridium thermoaceticum*: role of protonation of methyltetrahydrofolate in the mechanism of methyl transfer. *Biochemistry* 1999;38:5736–5745. [PubMed: 10231524]
78. Doukov T, et al. Crystal structure of a methyltetrahydrofolate and corrinoid dependent methyltransferase. *Structure* 2000;8:817–830. [PubMed: 10997901]
79. Svetlitchnaia T, et al. Structural insights into methyltransfer reactions of a corrinoid iron-sulfur protein involved in acetyl-CoA synthesis. *Proc Natl Acad Sci USA* 2006;103:14331–14336. [PubMed: 16983091]
80. Smith AE, et al. Protonation state of methyltetrahydrofolate in a binary complex with cobalamin-dependent methionine synthase. *Biochemistry* 2000;39:13880–13890. [PubMed: 11076529]
81. Zhao S, et al. Mechanistic studies of the methyltransferase from *Clostridium thermoaceticum*: origin of the pH dependence of the methyl group transfer from methyltetrahydrofolate to the corrinoid/iron-sulfur protein. *Biochemistry* 1995;34:15075–15083. [PubMed: 7578120]
82. Matthews RG. Cobalamin-dependent methyltransferases. *Acc Chem Res* 2001;34:681–689. [PubMed: 11513576]
83. Menon S, et al. The role of an iron-sulfur cluster in an enzymatic methylation reaction: methylation of CO dehydrogenase/acetyl-CoA synthase by the methylated corrinoid iron-sulfur protein. *J Biol Chem* 1999;274:11513–11518. [PubMed: 10206956]
84. Menon S, et al. Role of the [4Fe-4S] cluster in reductive activation of the cobalt center of the corrinoid iron-sulfur protein from *Clostridium thermoaceticum* during acetyl-CoA synthesis. *Biochemistry* 1998;37:5689–5698. [PubMed: 9548955]
85. Evans JC, et al. Structures of the N-terminal modules imply large domain motions during catalysis by methionine synthase. *Proc Natl Acad Sci USA* 2004;101:3729–3736. [PubMed: 14752199]
86. Taurog RE, et al. Synergistic, random sequential binding of substrates in cobalamin-independent methionine synthase. *Biochemistry* 2006;45:5083–5091. [PubMed: 16618097]
87. Peters JW, et al. X-ray crystal structure of the Fe-only hydrogenase (Cpl) from *Clostridium pasteurianum* to 1.8 angstrom resolution. *Science* 1998;282:1853–1858. [PubMed: 9836629]
88. Nicolet Y, et al. A novel FeS cluster in Fe-only hydrogenases. *Trends Biochem Sci* 2000;25:138–143. [PubMed: 10694885]

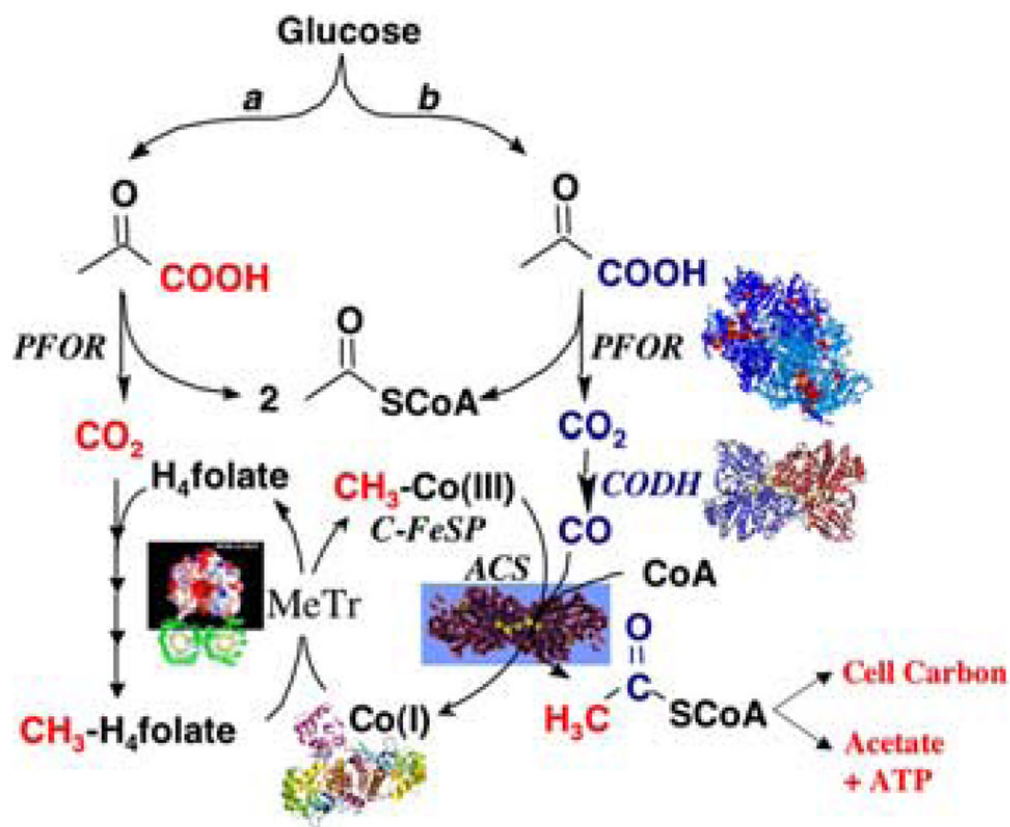


FIGURE 1. The Wood-Ljungdahl pathway with the Eastern and Western branches depicted in red and blue, respectively. (In color in *Annals* on line.)

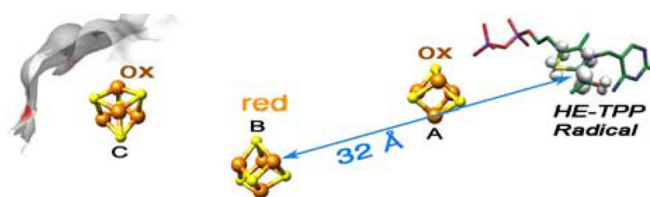


FIGURE 2. PFOR state including the HE-TPP radical, with the structure based on spectroscopic results, showing highly delocalized spin distribution (From Astashkin *et al.*²⁹ Used with permission.), and the distance from HE-TPP radical to coupled cluster. Location of the clusters is based on the structure (PDB 1KEK).

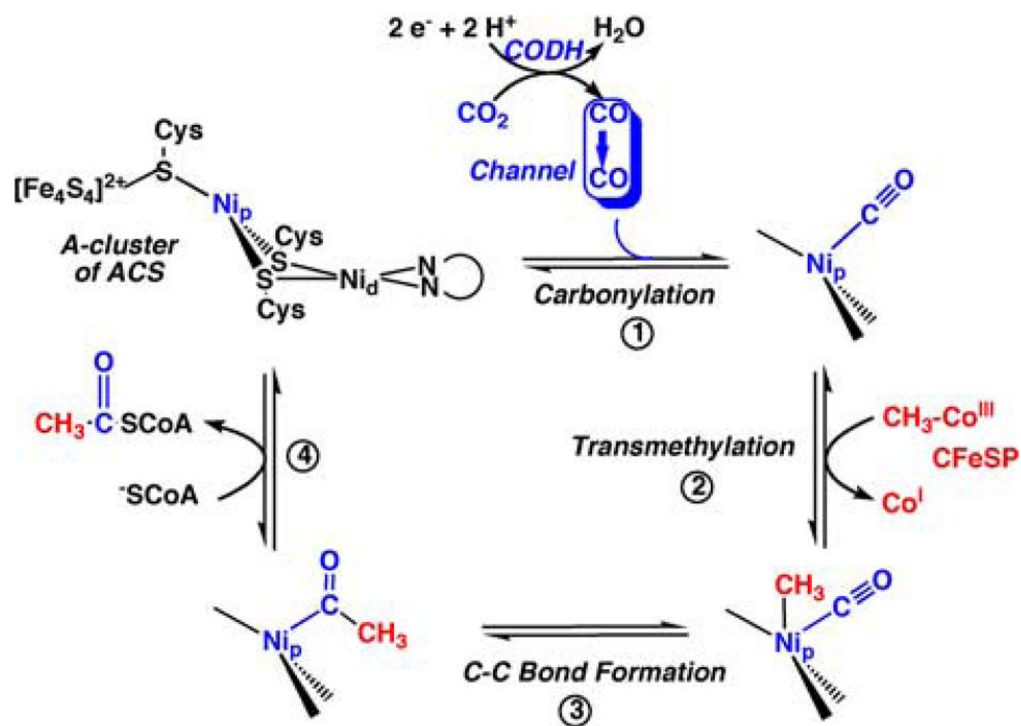


FIGURE 3. ACS mechanism emphasizing the organometallic nature of the reaction sequence and the channel to deliver CO from the CODH active site to the A-cluster.

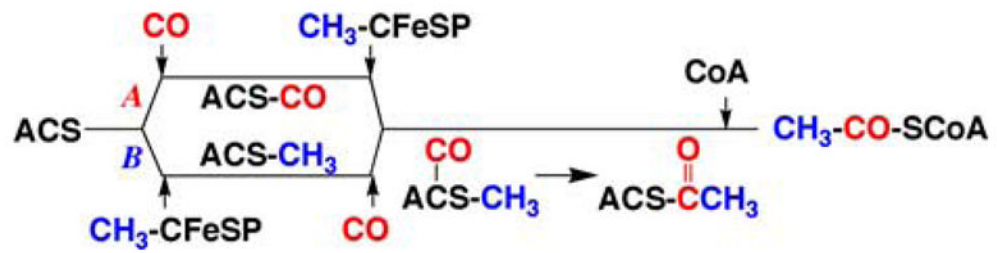


FIGURE 4.
Random mechanism of acetyl-CoA synthesis.

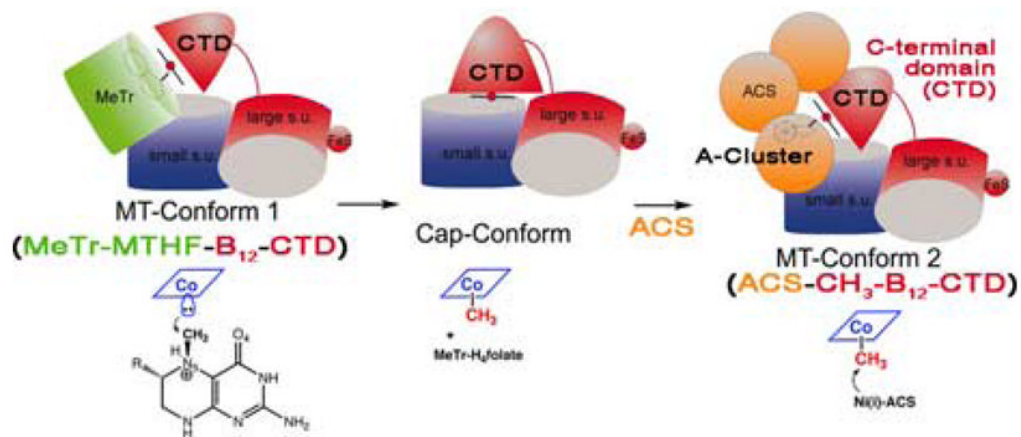


FIGURE 5. Proposed conformers and interactions of the CFeSP. (Modified from Svetlitchnaia *et al.*⁷⁹)